Inventory of Supplemental Information

Fig. S1 – Shows structures and *in vitro* efficacy of candidate compounds, and supports claims based on the data in Fig. 1 that DNPME has a wider ratio of toxic to therapeutic doses and is safe for prolonged treatment of rats.

Fig. S2 – Provides additional data to supplement Fig. 2 indicating that DNPME is effective at reversing NAFLD associated with reductions in DAG concentration without changes in a number of other mechanisms that have been implicated in insulin resistance.

Fig. S3 – Supports the conclusions drawn from the data in Fig. 3 that DNPME reverses hyperglycemia, hypertriglyceridemia, and NAFLD in two rat models of type 2 diabetes.

Fig. S4 – Shows additional data to compliment the findings shown in Fig. 4 indicating that DNPME promotes subtle hepatic uncoupling without measurable whole-body uncoupling at the doses given in these studies.

Supplemental Experimental Procedures – Additional information necessary to replicate certain techniques used in this study (animal care, chemical synthesis, LC/MS measurement of DNP and DNPME concentrations, *in vitro* oxygen consumption measurement, and flux studies) is presented in this section.

Supplemental References

Figure S1

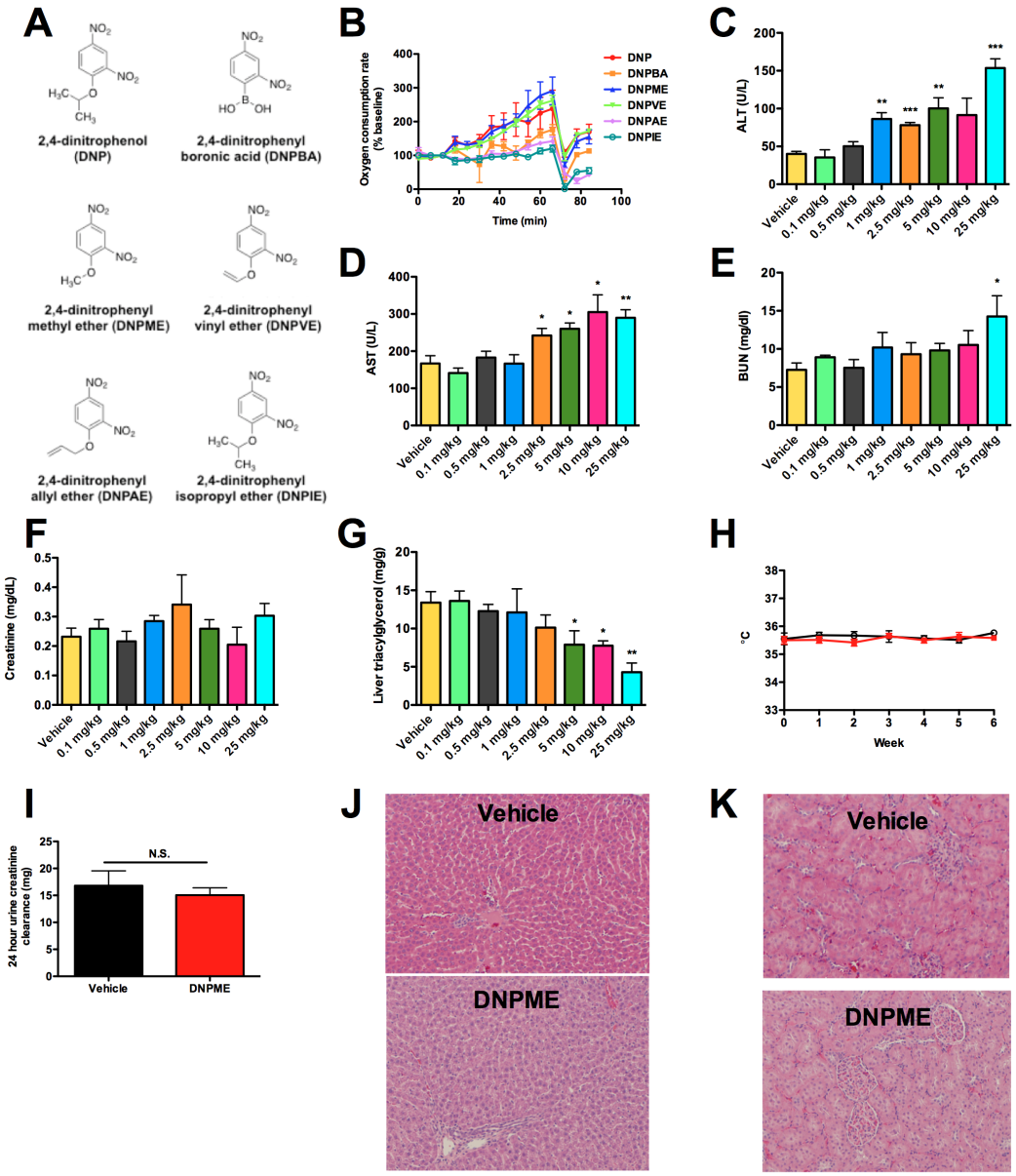

Supplemental Figure Legends

Figure S1. (A) Screening of candidate liver-targeted DNP compounds: structures of each candidate compound tested. (B) Basal oxygen consumption rate in plated hepatocytes, then oxygen consumption rate with addition of the candidate compounds at increasing doses. (C)-(G) ALT, AST, BUN, creatinine, and hepatic

TAG in rats treated for 5 days with DNP or vehicle. *P<0.05, **P<0.01, ***P<0.001. (H) Rectal temperature in rats treated for 6 weeks with DNPME or vehicle (red squares = DNPME, black circles = vehicle). (I) 24 hour urine creatinine clearance in rats treated for 6 weeks with DNPME or vehicle. (J)-(K) Representative images from liver and kidney, respectively, stained with hematoxylin & eosin. Data are mean ± SEM.

Figure S2

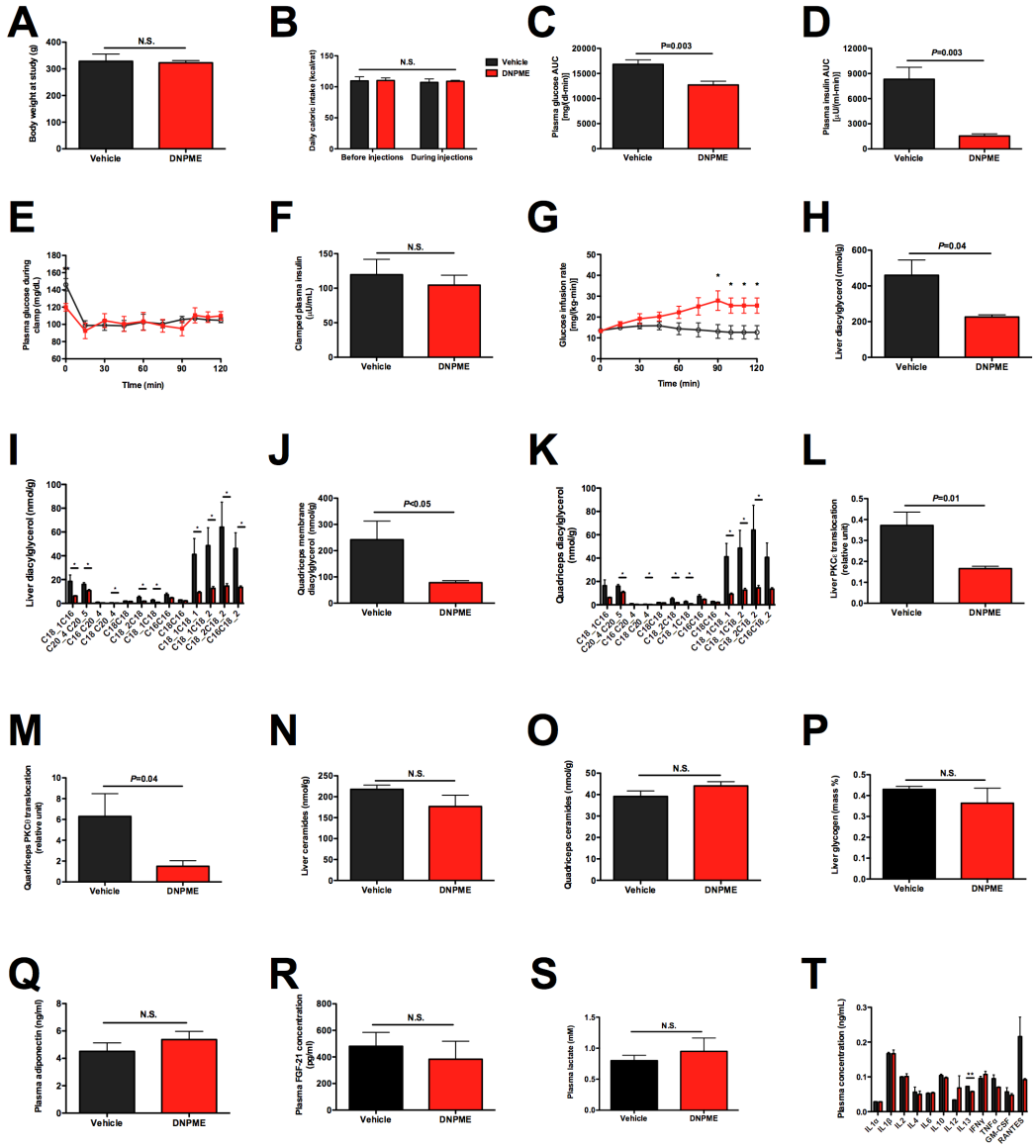

Figure S2. DNPME reverses NAFLD and insulin resistance. Rats used in these studies were fasted overnight (16 hours). (A) Body weight at the time of clamp. (B) Food intake before and during injections of DNPME or vehicle. (C), (D) Plasma glucose and insulin concentrations area under the curve during an intraperitoneal glucose tolerance test. (E) Plasma glucose during the hyperinsulinemic-euglycemic clamp. In panels (E) and (G), black circles = vehicle

treated, red squares = DNPME treated. (F) Plasma insulin concentrations at the end of the clamp. (G) Glucose infusion rate required to maintain euglycemia. (H), (I) Liver diacylglycerol and DAG species. (J), (K) Quadriceps DAG and DAG species. (L), (M) Liver and quadriceps PKCε and PKCθ translocation. (N), (O) Liver and muscle ceramide concentration. (P) Liver glycogen content. (Q), (R) Plasma adiponectin and FGF-21 concentrations. (S) Plasma lactate concentration. (T) Plasma concentration of inflammatory markers. n=3 per group. Unless otherwise specified, n=5-8 per group. *P<0.05, **P<0.01. Data are mean ± S.E.M.

Figure S3

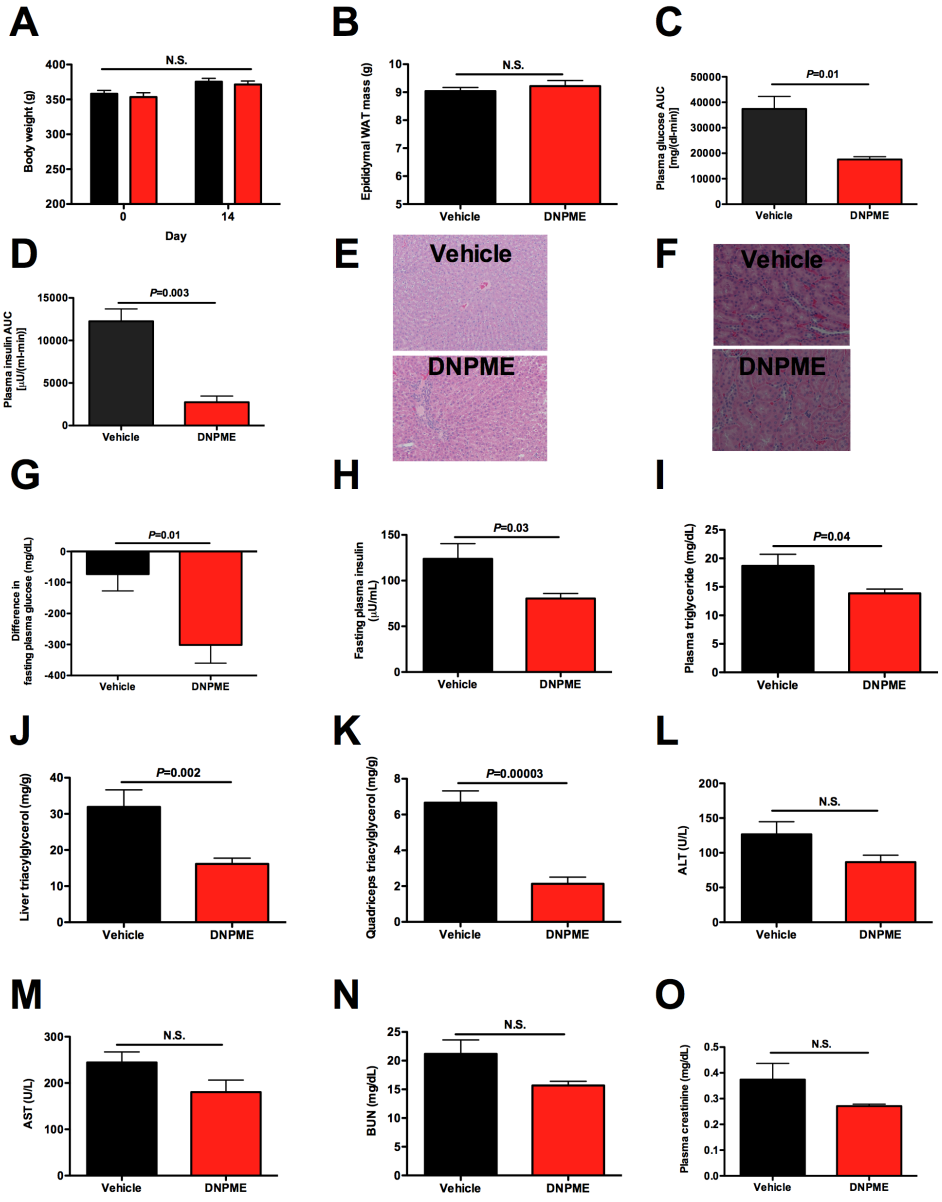

Figure S3. 14 days of DNPME treatment reverses hyperglycemia and improves insulin sensitivity in rat models of type 2 diabetes. (A)-(D) Rats treated with low dose streptozotocin treatment and 3-day high fat feeding. Body weight, WAT

weight, insulin and glucose area under the curve in an intraperitoneal glucose tolerance test. n=5-7 per group. (E)-(F) Liver and renal histology, respectively, in T2D rats. (G)-(O) Zucker Diabetic Fatty rats. Fasting plasma glucose, insulin, and triglycerides; liver and quadriceps triglycerides; plasma ALT, AST, BUN, and creatinine. n=6-8 per group. Data are presented as mean ± S.E.M.

Figure S4

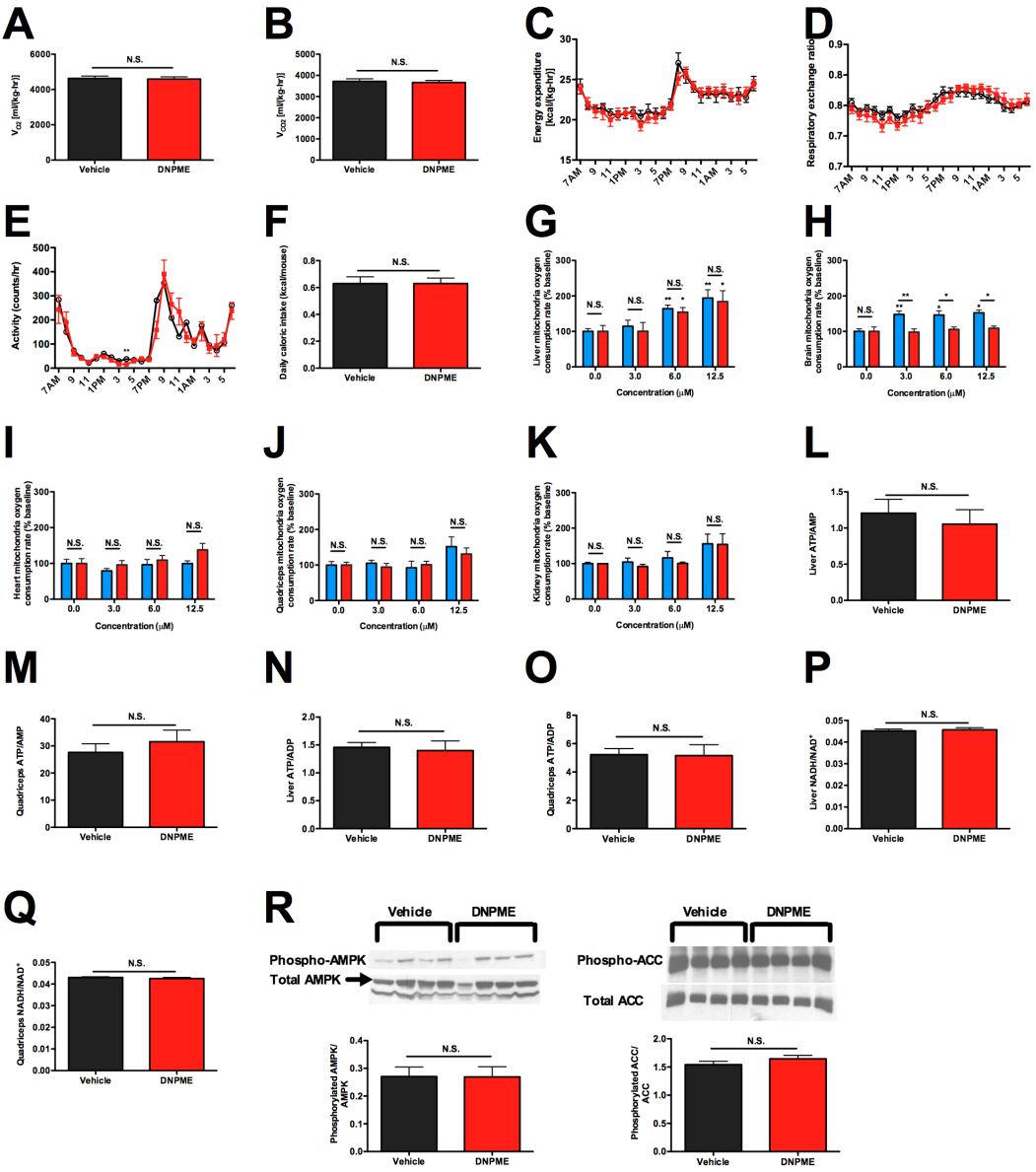

Fig. S4. Basal metabolism in DNPME treated mice and in 5 day DNPME-treated rats *in vitro*. (A) Oxygen consumption. (B) Carbon dioxide production. (C)-(E) Energy expenditure, respiratory exchange ratio, and activity throughout the day. Black circles = vehicle treated, red squares = DNPME treated. (F) Daily caloric

intake. n=8 per group in panels (A)-(F). (G)-(K) Oxygen consumption rate in isolated mitochondria obtained from liver, brain, heart, quadriceps and kidney after the addition of varying doses of DNP (blue) or DNPME (red). The mitochondria were incubated throughout the experiment with substrate, ADP, and oligomycin to create State 4 respiration. Statistics over individual bars refer to differences from oxygen consumption rate at 0 μM by 2-tailed paired t-test. If statistics are not listed over certain bars, there was no significant difference from 0 μM. In all panels, $*P<0.05$, $**P<0.01$. (L) Liver ATP/AMP. (M) Quadriceps ATP/AMP, (N) Liver ATP/ADP, (O) Quadriceps ATP/ADP. (P) Liver $NADH/NAD^+$. (Q) Quadriceps $NADH/NAD^+$. (R) Liver AMPK phophosphorylation relative to total AMPK, and ACC phosphorylation relative to total ACC. For panels (G)-(R), n=4-7 per group. Data are shown as mean ± S.E.M.

Supplemental Experimental Procedures

Animals

Unless otherwise noted, animals were fed normal chow (Harlan 2018 [58% calories from carbohydrate, 24% from protein, 18% from fat]). Where specified, animals were fed safflower oil based high fat diet (Dyets) with 60% calories from fat. All animals had *ad libitum* access to water at all times. Where specified, caloric intake was enriched by free access to 5% sucrose water. Rats used for experiments requiring blood collection underwent surgery under isoflurane anesthesia to place catheters in the jugular vein and internal carotid artery. Another group of rats underwent surgery to place catheters in the antrum of the stomach. All animals were allowed to recover for at least 1 week before any further experiments were performed.

Rats used for the studies to determine whether DNPME could prevent the development of NAFLD were fed high fat diet and sucrose water for 2 weeks, during which time they were concurrently injected with daily 5 mg/kg IP doses of DNPME in 100% DMSO (250 µl/kg body weight) or vehicle. Rats used for the NAFLD reversal studies were fed high fat diet and sucrose water for 1 week, then were given daily injections of DNPME or vehicle for 5 days while continuing the high fat diet and sucrose water. To measure caloric intake, the volume of water and weight of food consumed each day were measured, and calorie content was calculated using the known composition of each item.

To induce a mild beta-cell defect and type 2 diabetes, rats were injected with 75 mg/kg nicotinamide and, following a 15 minute wait, 60 mg/kg streptozotocin. Animals were allowed to recover for 3 days, and those with random plasma glucose between 150 and 350 mg/dl were used for further study. At this time, high fat diet and sucrose water feeding was initiated. After 3 days of feeding, two weeks of daily DNPME or vehicle injections were begun.

General experimental procedures for chemical synthesis

NMR Spectra were measured at ambient temperature unless otherwise noted. ^{1}H NMR spectra were recorded on either a 500 or 400 MHz Bruker spectrometer. Chemical shifts are reported in ppm (δ) relative to tetramethylsilane, using the solvent as a reference ($CDCl_3$ = 7.26 ppm). The following is an example data point: chemical shift (multiplicity [s = singlet, d = doublet, t = triplet, q = quartet, m = multiplet, br = broad, and combinations thereof], coupling constants [Hz], integration). ^{13}C NMR spectra were recorded on a 500 MHz (126 MHz) or 400 MHz (101 MHz) Bruker spectrometer with complete proton decoupling. Chemical shifts are reported in ppm (δ) relative to tetramethylsilane using the solvent as a reference ($CDCl_3$ = 77.16 ppm). MS data were obtained with an Agilent 6890/5973 GC/MSD System. Yield refers to isolated material.

Synthesis of candidate compounds

2,4-Dinitrophenyl boronic acid (DNPBA; 3) was prepared as previously described (Collibee and Yu, 2005).

2,4-Dinitrophenyl methyl ether (DNPME; 4)

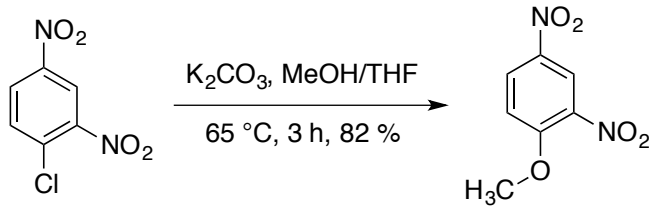

5 **4**

The title compound was synthesized according to a literature procedure (Gong et al., 2002) with minor modifications. Briefly, 5 (4.05 g; 20 mmol) was dissolved in MeOH/THF (3.2 ml/2 ml), treated with K_2CO_3 (4.70 g; 34 mmol) and heated at 65 °C for 3 h in a sealed tube. The reaction mixture was then diluted with dichloromethane (50 ml) and washed twice with 3 % $NaHCO_3$ solution. The organic layers were combined, dried over Na_2SO_4 and concentrated to afford pure 4 as a pale yellow solid (3.25 g; 82 %). ^{1}H NMR (400 MHz, $CDCl_3$) δ 8.74 (d, *J* = 2.8, 1H), 8.45 (dd, *J* = 9.3, 2.8, 1H), 7.24 (d, *J* = 9.2, 1H), 4.10 (s, 3H); ^{13}C NMR (101 MHz, $CDCl_3$) δ 157.43, 140.27, 138.95, 129.29, 122.02, 113.78, 57.62; IR (film, cm^{-1}) 3101, 1598, 1520, 1342, 1279; MS (e.i.) m/z 198 [M^+, 42%].

2,4-Dinitrophenyl vinyl ether (DNPVE; 6)

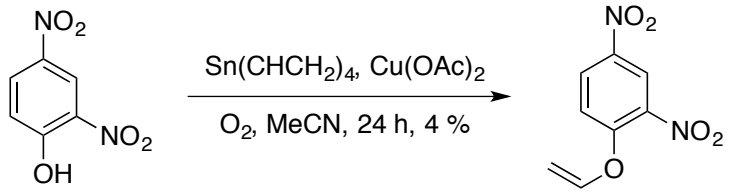

1 **6**

The title compound was prepared from 2,4-dinitrophenol (1, 184 mg; 1 mmol), following a published protocol (Blouin and Frenette, 2001). After SiO_2 chromatography (10-30 % EtOAc/hexane), 5 was obtained as a pale yellow gum (9 mg; 4 %). ^{1}H NMR (400 MHz, $CDCl_3$) δ 8.80 (d, *J* = 2.7, 1H), 8.44 (dd, *J* = 9.2, 2.8, 1H), 7.33 (d, *J* = 9.2, 1H), 6.68 (dd, *J* = 13.5, 5.9, 1H), 5.18 (dd, *J* = 13.4, 2.6, 1H), 4.93 (dd, *J* = 5.8, 2.5, 1H); ^{13}C NMR (101 MHz, $CDCl_3$) δ 154.44, 145.03, 141.93, 139.38, 129.07, 122.18, 117.75, 102.77; IR (film, cm^{-1}) 1600, 1527, 1338, 1264; MS (e.i.) m/z 180 [$(M - NO)^+$, 7%].

2,4-Dinitrophenyl allyl ether (DNPAE; 7)

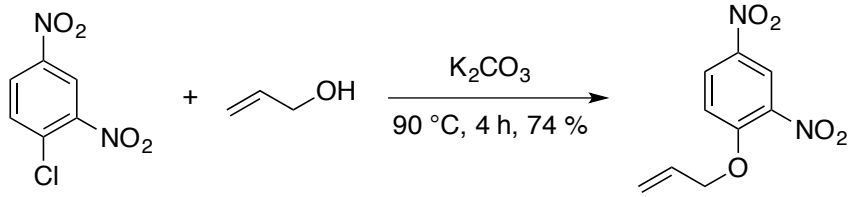

5 **7**

The title compound was synthesized from 5 (4.05 g; 20 mmol), using an identical method as described above for 4, substituting allyl alcohol (5.4 ml) for MeOH/THF, and obtained as a pure 7 as a yellow solid (3.297 g; 74%). ^{1}H NMR (400 MHz, $CDCl_3$) δ 8.72 (d, *J* = 2.8, 1H), 8.40 (dd, *J* = 9.2, 2.8, 1H), 7.22 (d, *J* = 9.2, 1H), 6.03 (ddt, *J* = 17.3, 10.3, 5.0, 1H), 5.51 (dq, *J* = 17.3, 1.6, 1H), 5.40 (dq,

J = 10.7, 1.4, 1H), 4.83 (dt, *J* = 5.0, 1.6, 2H); ^{13}C NMR (101 MHz, $CDCl_3$) δ 156.41, 140.19, 139.09, 130.41, 129.09, 121.97, 119.64, 114.92, 71.02; IR (film, cm^{-1}) 1604, 1521, 1488, 1340, 1313, 1279, 1242; MS (e.i.) m/z 224 [M^+, 3%].

2,4-Dinitrophenyl isopropyl ether (DNPIE; 8)

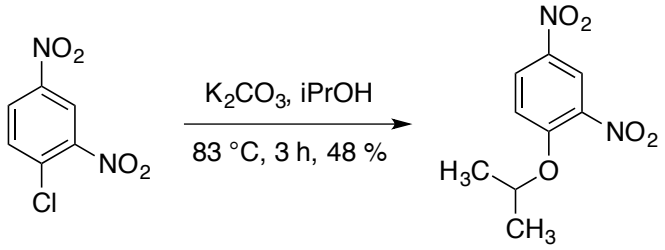

5 **8**

The title compound was synthesized from 5 (1.02 g; 5 mmol), using an identical method as described above for 4, substituting i-PrOH (1.5 ml) for MeOH/THF, and obtained as a yellow solid (542 mg; 48 %). ^{1}H NMR (500 MHz, $CDCl_3$) δ 8.67 (d, *J* = 2.8, 1H), 8.39 (dd, *J* = 9.3, 2.8, 1H), 7.19 (d, *J* = 9.4, 1H), 4.85 (hept, *J* = 6.0, 1H), 1.46 (d, *J* = 6.0, 6H); ^{13}C NMR (126 MHz, $CDCl_3$) δ 156.05, 139.87, 139.71, 128.82, 121.93, 115.17, 74.32, 21.77; IR (film, cm^{-1}) 1604, 1521, 1486, 1340, 1311, 1282; MS (e.i.) m/z 226 [M^+, 3%].

2,4-Dinitrophenyl methyl ether-d6 (DNPME-d6; 9)

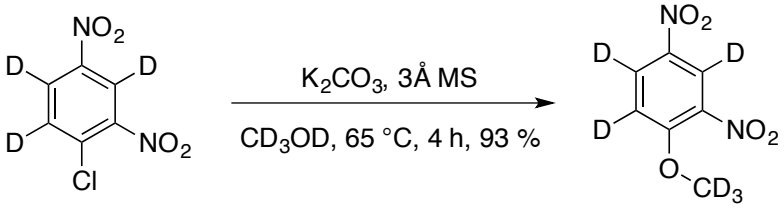

2 **9**

The title compound was synthesized using the same procedure as for compound 4, but with minor modifications. Briefly, 3Å molecular sieves and K_2CO_3 (92 mg; 0.66 mmol) were added to a microwave vessel and flame-dried. To this were added 2 (80 mg; 0.39 mmol) and CD_3OD (0.6 ml), and the reaction mixture was heated at 65 °C for 4 h in a microwave. The crude product was purified as described for 4 to afford 9 (74 mg; 93 %). ^{13}C NMR (126 MHz, $CDCl_3$) δ 157.44, 140.01, 138.71, 128.96 (t, *J* = 26.0), 121.68 (t, *J* = 26.2), 113.52 (t, *J* = 25.5), 56.84 (hept, *J* = 22.3); IR (film, cm^{-1}) 2308, 1579, 1518, 1425, 1372, 1336, 1305, 1248; MS (e.i.) m/z 204 [M^+, 20%].

NMR Spectral Data for Candidate Compounds

^1H NMR spectrum of 4

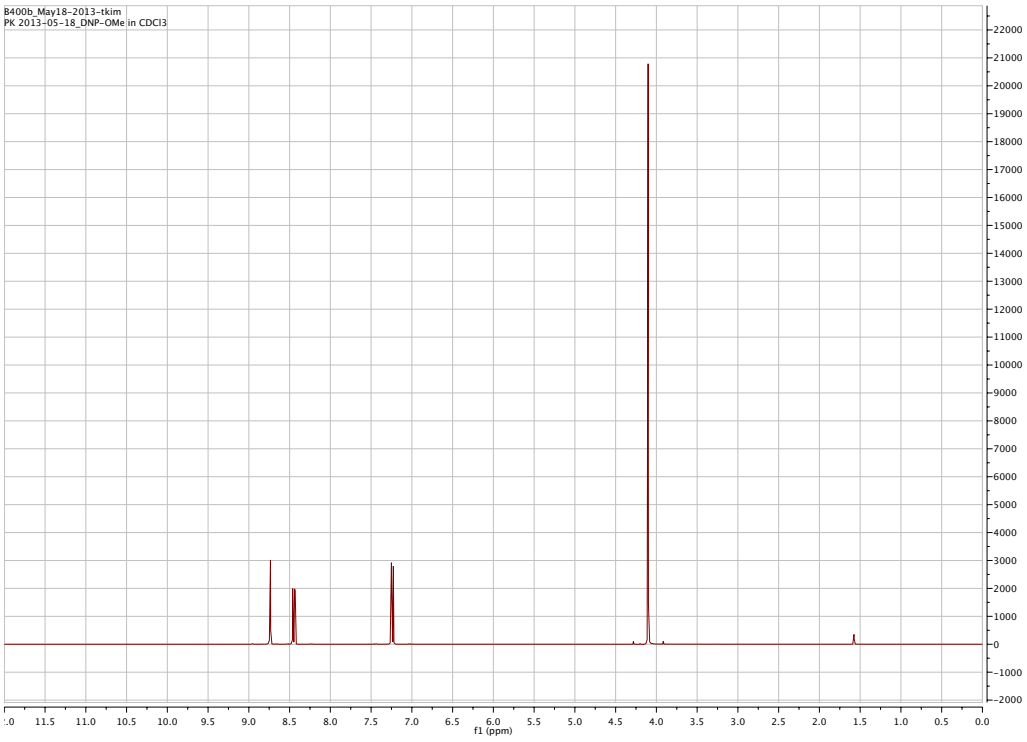

^{13}C NMR spectrum of 4

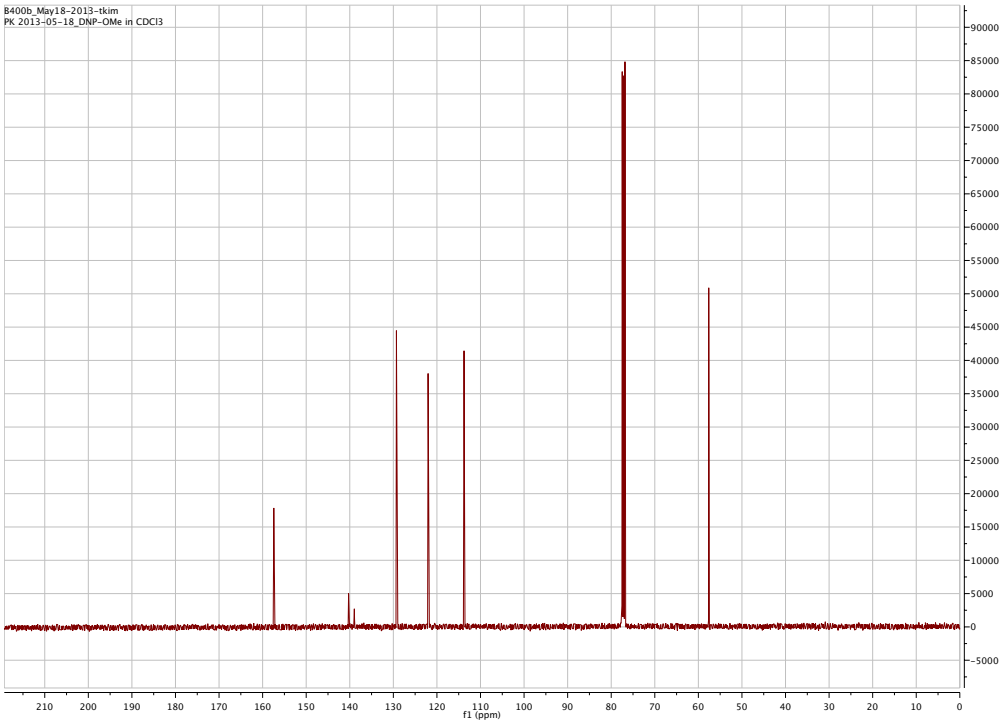

^{1}H NMR spectrum of 6

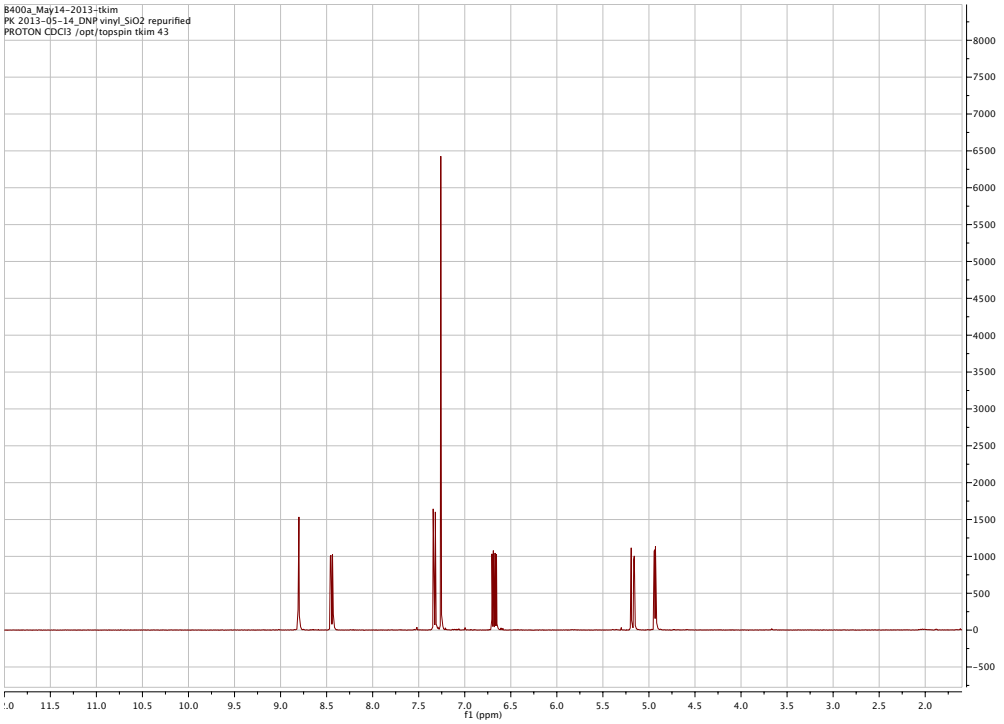

^{13}C NMR spectrum of 6

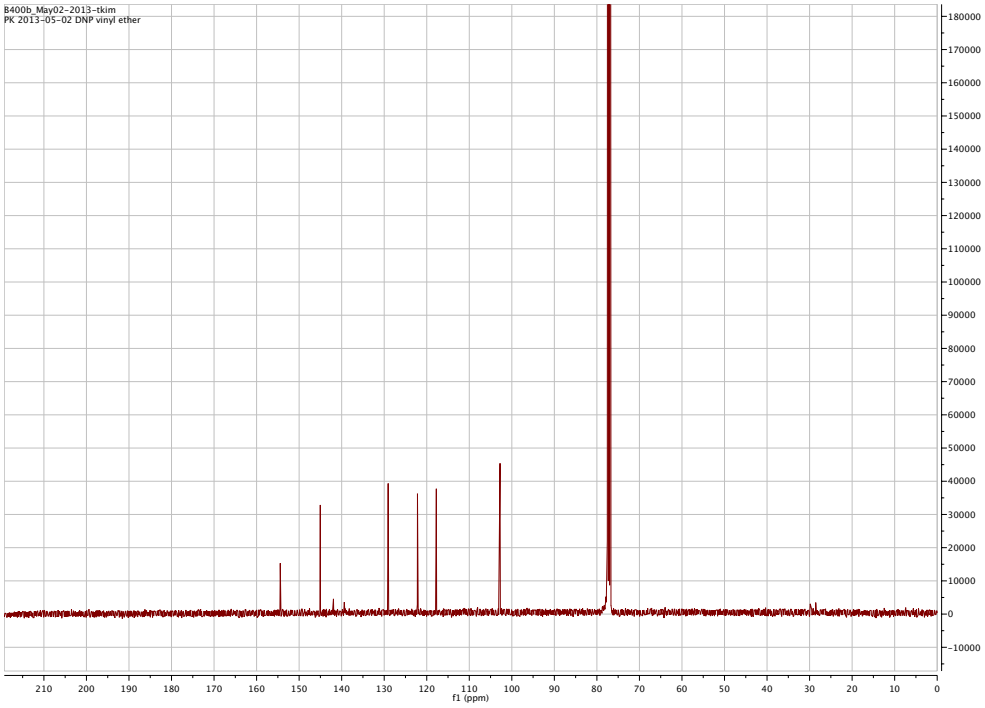

^{1}H NMR spectrum of 7

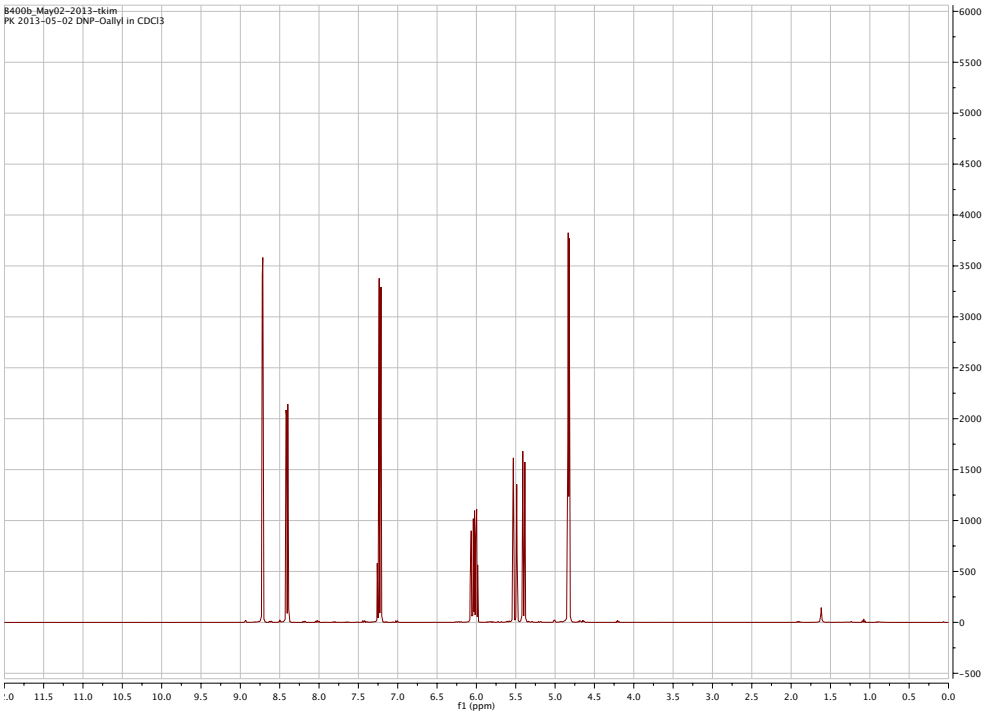

^{13}C NMR spectrum of 7

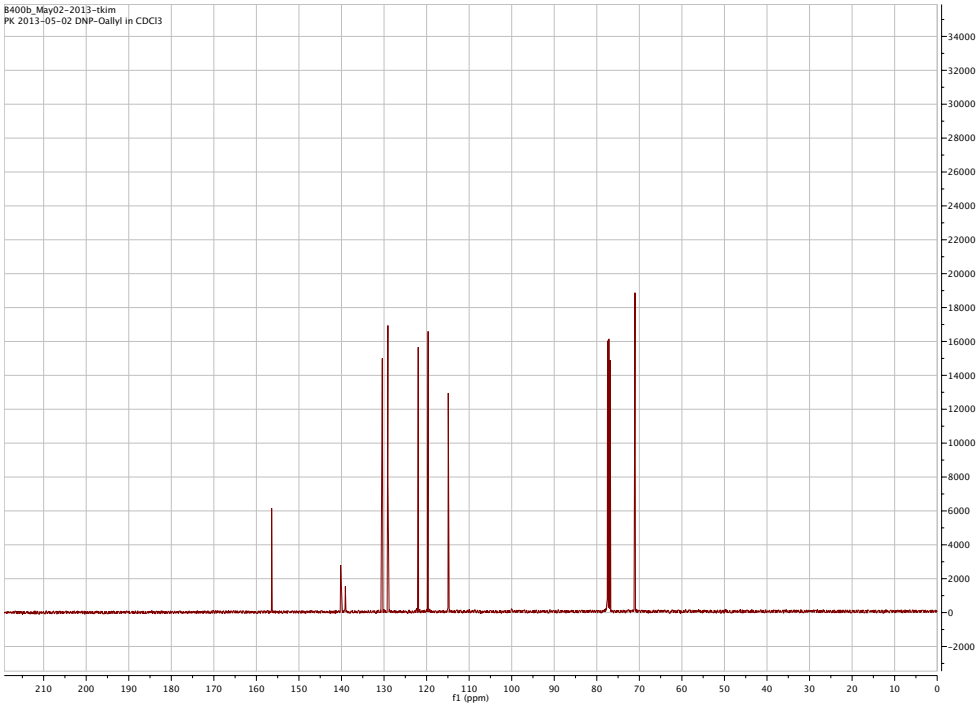

^{1}H NMR spectrum of 8

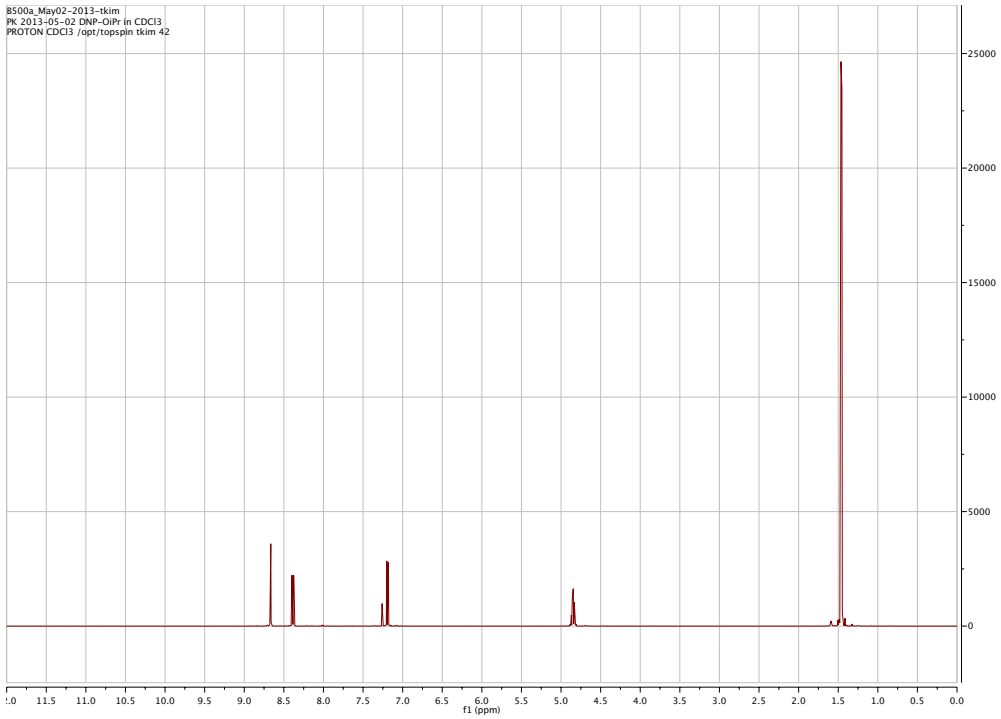

^{13}C NMR spectrum of 8

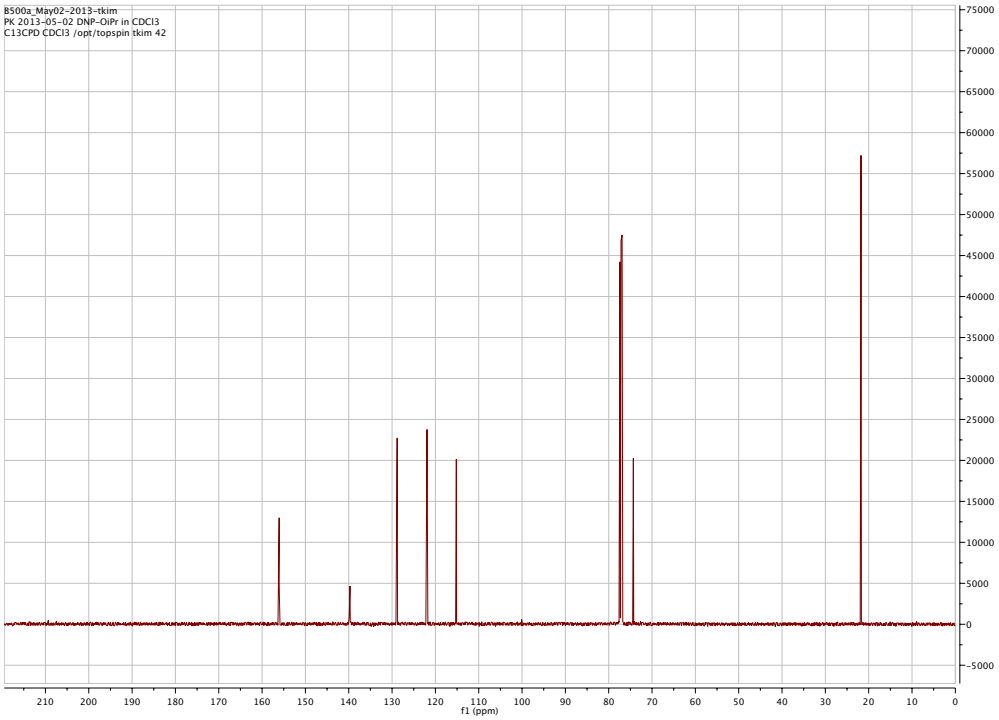

^{13}C NMR spectrum of 9

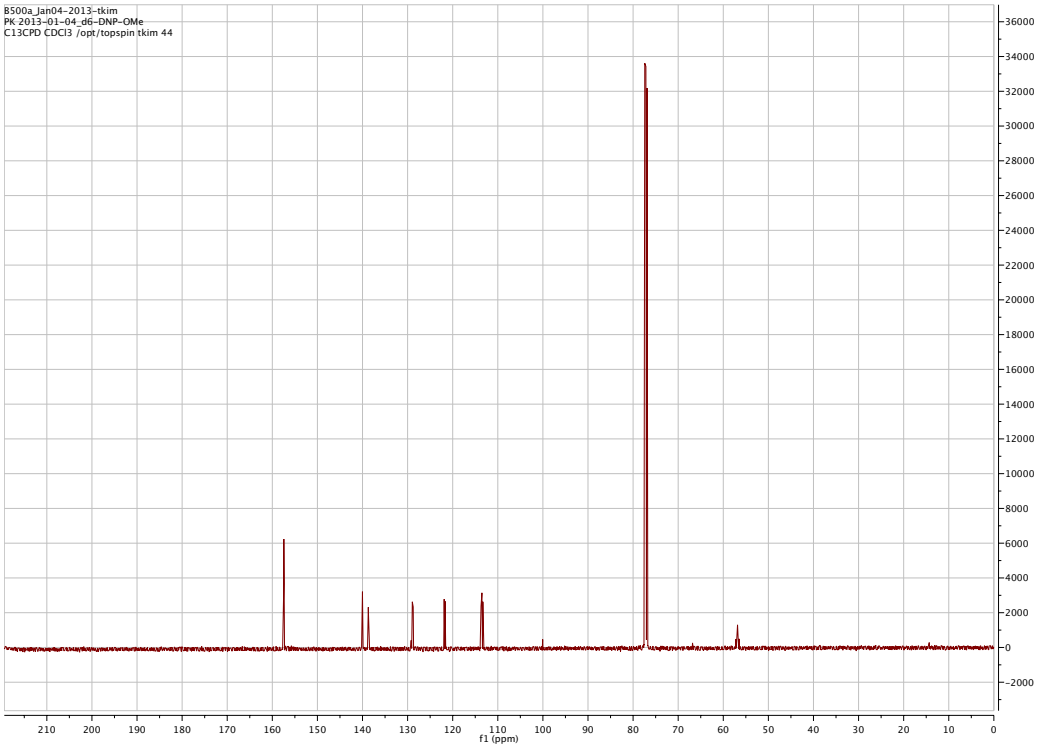

Measurement of plasma DNP and DNPME concentrations

LC/MS/MS method development and analysis were performed on the Applied Biosystems 4000 QTRAP, equipped with a Shimadzu ultra fast liquid chromatography (UFLC) system. Electrospray ionization (ESI) source with negative-ion detection was shown as the most sensitive for both qualitative and quantitative analysis of DNP and DNPME. The quantitative analysis of DNP was monitored in MRM mode with an ion pair (183.0/109.0). The optimized parameters are: curtain gas 25; collision gas 9, probe temperature 480 ^{0}C; ion source gas 1 20; ion source gas 2 25; declustering potential (DP) -45 V; entrance

potential (EP) -10 V; collision energy (CE) -35 V and collision cell exit potential -12 V.

The molecular radical anion of DNPME is unstable at the ionization temperature due to the labile methyl-oxygen ether bond, but the fragmented DNP anion is one of the most abundant peaks for DNPME using the parameters optimized for DNP, thus both DNP and DNPME can be quantitated by the same method. A Hibar LiChrosorb analytical HPLC column (RP-C8, 4 x 125 mm, particle size 5μM) (Merck KGaA) is used to separate DNP and DNPME using an isocratic flow (250 μl/min) of 15% 10 mM ammonium formate and 85% methanol/water (95/5). The retention time is about 4 min for DNP, and about 7 min for DNPME. Deuterated 2,4-dinitrophenol (DNP-D_3) and deuterated DNP-methyl ether (DNPME-D_6) were used as the internal standards for DNP and DNPME quantitation, respectively.

Extraction from plasma samples for LC/MS/MS analysis

Plasma samples (10-100 μL) were mixed with 2.0 ml pre-chilled chloroform/methanol (v/v: 2/1) containing 0.01% BHT in 5 ml glass vials, then added 250 μl water together with 10 nmol DNP-D_3 and 10 nmol DNPME-D_6 as the internal standards. The mixtures were vortexed for 10 seconds before centrifugation at 4000 rpm for 10 min. The bottom organic layer was carefully collected and dried with a steady stream of nitrogen gas. The residual was reconstituted in 200 μl methanol for LC/MS/MS analysis for DNP and/or DNPME metabolites.

Screening of candidate compounds

Primary hepatocytes were isolated by the Yale Liver Center as previously described (Neufeld, 1997) and plated on a collagen-coated 24-well plate (Seahorse Bioscience). After a 6-hour incubation, cells were transferred to the Seahorse XF Analyzer for measurement of oxygen consumption rate. Basal oxygen consumption was measured, then sequential additions of DNP (positive control) or the candidate compounds raised the concentration of the putative uncoupler to 10, 100, 500, and 1000 μM. Absolute oxygen consumption rates were normalized to the oxygen consumption rate measured before the first addition of uncoupler.

Extraction from tissue samples for LC/MS/MS analysis

Frozen tissue samples (~100 mg) were weighed and suspended in 2 ml microcentrifuge tubes with 1.6 ml pre-chilled chloroform/methanol (v/v: 2/1) containing 0.01% BHT and one metal bead, and then added 10 nmol DNP-D_3 (Cambridge Isotopes) and 10 nmol DNPME-D_6 (synthesized as described above) as the internal standards. The tissue samples were disrupted with Qiagen TissueLyser at 30 Hz for 15 min, and then transferred into 5 ml glass vials, followed by addition of 0.5 ml chloroform and 250 μl water into each samples. The samples were centrifuged at 4000 rpm for 10 min after vortexed for 10 seconds. The bottom organic layer was collected and dried with a gentle flow of

nitrogen. The residual was reconstituted in 200 µl methanol for LC/MS/MS analysis of DNP and/or DNPME metabolites.

Respiration studies

Tissues isolated from overnight-fasted rats were homogenized on ice in 10-20x volume of isolation buffer containing 215 mM mannitol, 75 mM sucrose, 0.1% BSA, 1 mM EGTA, 20 mM HEPES at pH 7.2, and centrifuged for 10 min at 1000g. The supernatant was then isolated and centrifuged for 10 min at 8000g. After the high-speed centrifugation, the pellet was resuspended in BSA-free isolation buffer and washed by centrifugation. A Bradford assay was used to measure the protein concentration of each mitochondrial sample. Samples were diluted to 2 mg/ml with BSA free isolation buffer and stored on ice for further study. The Seahorse XF24 Analyzer (Seahorse Biosciences) was used to measure mitochondrial respiration in samples plated at 10 µg/well in respiration buffer (215 mM mannitol, 75 mM sucrose, 3 mM $MgCl_2$, 2.5 mM inorganic phosphates, 0.1% BSA, 25 mM MOPS, 10 mM pyruvate, 2.5 mM malate, 2.5 mM glutamate, 5 mM succinate, 2 mM ADP, and 1 µg/ml oligomycin at pH 7.2). Oxygen consumption was measured before and after the addition of DNP or DNPME (0, 3.125, 6.25, and 12.5 µM).

Measurement of tissue energetics

Livers from rats sacrificed by decapitation were isolated within 15 seconds, and quadriceps muscle within 40 seconds. ~50 mg of tissue were homogenized

in a buffer of 50% methanol, 10 μM EDTA, 2 mM ammonium acetate, and 20 μM d4 taurine. Following a 20 minute spin at 20,000 rcf and 4^{o} C, the supernatant was kept on ice for 20 min, then spun again at 16,000 rcf in filter tubes for 5 min. The flow-through was separated on a C18 5-μm 100 Å 4.6 × 100-mm column (Phenomenex) before ionization for multiple reaction monitoring analysis by LC/MS/MS (Applied Biosystems/MDS SCIEX, 5000 Q-TRAP). Each analyte was eluted isocratically in 12 uM ammonium formate/5% methanol at a flow rate of 400 μl/min. Individual ion pairs were designated for each analyte, and the relative concentrations were determined by manual integration.

Metabolic flux studies

Measurement of hepatic positional metabolite enrichment

To measure total glutamate enrichment from livers of rats infused with [3-^{13}C] lactate, ~100 mg frozen liver were homogenized in 400 μL ice-cold 50% acetonitrile. The samples were centrifuged at 10,000 g for 10 min, and the supernatant was isolated. After overnight storage at 4°C, the samples were centrifuged at 10,000 g for 10 min through a Nanosep 100k Omega filter (Pall Life Sciences). The flow-through was separated on a hypercarb column (Thermo Scientific; 4.6 x 100 mm; 5 μm particle size) before ionization for multiple reaction monitoring analysis by LC/MS/MS (Applied Biosystems MDS SCIEX, 4000 Q-TRAP).

To measure positional glutamate and alanine enrichment, the liver samples were extracted for nuclear magnetic resonance (NMR) spectroscopy. ~4-6 g ground liver were centrifuged in ~30 mL 7% perchloric acid. The pH of the supernatant was adjusted to 6.5-7.5 using 30% potassium hydroxide and 7% perchloric acid as needed, and the extract was dehydrated by lyophilizing for 2-3 days. The extract was resuspended in 500 µL potassium phosphate buffer: 2.4 mM NaCOOH, 30 mM K_2HPO_4, 10 mM KH_2PO_4, 20 mM DMSO (internal standard) in 100% D_2O. ^{13}C NMR spectra were collected using the AVANCE 500-MHz NMR spectrometer (Bruker Instruments). Spectra were acquired with relaxation time = 1 s, dummy scans = 32, and number of scans = 8,192 per block x 3 blocks. Correction factors for differences in T_1 relaxation times were determined from fully relaxed spectra of natural abundance glutamate and glucose solutions. The total glutamate enrichment by LC/MS/MS was divided algebraically according to the peak areas of [^{13}C] glutamate for each carbon corrected for T_1 relaxation times.

Total glucose enrichment in the NMR extract was determined by derivatizing 20 µL of the NMR extract with 100 µL methanol, then drying overnight in a Speed-Vac. The extract was then resuspended in 75 µL 1:1 acetic anhydride:pyridine and heated for 20 min at 65°C. The sample was cooled and quenched with 25 µL methanol. The total m+1 glucose enrichment of each sample was measured by gas chromatography/mass spectrometry as we have reported (Shulman et al., 1985). m+2, m+3, m+4, m+5, and m+6 enrichment were found to be negligible (<5% of m+1 enrichment at steady-state). ^{13}C NMR

spectra were used to determine relative concentrations of [^{13}C] glucose. As for glutamate, the total glucose enrichment by mass spectrometry was divided algebraically to measure the enrichment at each glucose carbon.

To measure positional alanine enrichment from [3-^{13}C] lactate infused rat livers, liver samples were extracted for NMR as described above, and the enrichment at [2-^{13}C] and [3-^{13}C] alanine was measured by proton-observed, carbon-edited NMR as we have reported (Alves et al., 2011).

Measurement of absolute hepatic flux rates

Livers from rats infused with [3-^{13}C] lactate and [^{3}H] glucose were extracted with perchloric acid as described by Alves et al. (2011). Basal glucose turnover was measured as described by Maggs (1998); as these rats were overnight fasted with low hepatic glycogen concentrations (Fig. S2P), all glucose production was presumed to be from gluconeogenesis. We assumed that gluconeogenesis was 90% hepatic and 10% renal; from our whole-body gluconeogenesis data, we could then calculate absolute hepatic gluconeogenesis. [3-^{13}C] lactate infusion allows us to measure the percent gluconeogenesis from pyruvate (flux through pyruvate carboxylase, V_{PC}) according to the equation $Gluconeogenesis\ from\ pyruvate = \frac{[1-^{13}C] + [2-^{13}C]+[5-^{13}C]+[6-^{13}C]\ glucose}{2*([2-^{13}C]+[3-^{13}C]\ glutamate)}$. We can express flux through PC relative to TCA cycle flux, accounting for pyruvate cycling through pyruvate kinase and malic enzyme, as $\frac{V_{PC}}{V_{TCA}} = \frac{[2-^{13}C]\ glutamate-[4-^{13}C]\ glutamate}{([2-^{13}C]\ glutamate+[3-^{13}C]\ glutamate)-([2-^{13}C]\ alanine+[3-^{13}C]\ alanine)}$; because we

had previously calculated absolute V_{PC} as described above, we could back-calculate V_{TCA} from these data. Finally, $\frac{V_{PDH}}{V_{TCA}} = \frac{[4-^{13}C]\ glutamate}{[3-^{13}C]\ alanine}$; from the calculated V_{TCA}, we could determine V_{PDH} using this equation, and could measure the contribution of fatty acid oxidation to the TCA cycle as the difference between V_{TCA} and V_{PDH}.

Supplemental References

Alves, T.C., Befroy, D.E., Kibbey, R.G., Kahn, M., Codella, R., Carvalho, R.A., Falk Petersen, K., and Shulman, G.I. (2011). Regulation of hepatic fat and glucose oxidation in rats with lipid-induced hepatic insulin resistance. Hepatology *53*, 1175–1181.

Blouin, M., and Frenette, R. (2001). A new method for the preparation of aryl vinyl ethers. The Journal of Organic Chemistry.

Collibee, S.E., and Yu, J. (2005). A facile and convenient synthesis of functionalized ortho-nitrophenylboronic acids. Tetrahedron Letters.

Gong, G., Gao, X., Wang, J., Zhao, D., and Freeman, H.S. (2002). Trisazo Direct Black dyes based on nonmutagenic 3, 3′-disubstituted benzidines. Dyes and Pigments.

Hutter, E., Renner, K., Pfister, G., Stöckl, P., Jansen-Dürr, P., and Gnaiger, E. (2004). Senescence-associated changes in respiration and oxidative phosphorylation in primary human fibroblasts. Biochem. J. *380*, 919–928.

Kuznetsov, A.V., Strobl, D., Ruttmann, E., Königsrainer, A., Margreiter, R., and Gnaiger, E. (2002). Evaluation of mitochondrial respiratory function in small biopsies of liver. Anal. Biochem. *305*, 186–194.

Maggs, D.G., Buchanan, T.A., and Burant, C.F. (1998). Metabolic effects of troglitazone monotherapy in type 2 diabetes mellitusa randomized, double-blind, placebo-controlled trial. Ann. Intern. Med*. 128*, 176-185.

Shulman, G.I., Ladenson, P.W., Wolfe, M.H., Ridgway, E.C., and Wolfe, R.R. (1985). Substrate cycling between gluconeogenesis and glycolysis in euthyroid, hypothyroid, and hyperthyroid man. J. Clin. Invest. *76*, 757–764.